A novel nonlinear controller design of three-phase grid-tied photovoltaic system

Fatim-Zahra Zaghar[1], Zineb Hekss[2], Mohamed Rafi[3], Salwa Echalih[2], Abdrraouf Ridah[1]
[1]LIMAT Lab, Faculty of Sciences Ben M'sick, Hassan II University, Casablanca, Morocco
[2]ESE Lab, ENSEM of Casablanca, Hassan II University, Casablanca, Morocco
[3]Industrial Engineering Lab, Mohammed VI International Academy of Civil Aviation, Casablanca, Morocco

Article Info

ABSTRACT

This paper explores the challenges associated with the control of a two-stage three-phase electrical grid connected to a photovoltaic (PV) system. The core control objectives encompass: i) Maximizing the utilization of available power from the PV panel; ii) Regulating the DC-link voltage to a predetermined reference; and iii) Ensuring power factor correction (PFC) on the grid side. To achieve these objectives, two loops nonlinear controller are developed. In the outer loop, the duty cycle of a boost converter is controlled using integral backstepping technique with the perturb & observe (P&O) algorithm, which provides reference voltages to track maximum power points, and Lyapunov theory to ensure the system's stability. In addition, the Inner loop is designed using proportional integrator (PI) controller to ensure the unit power factor correction. An assessment of the proposed method is conducted through a comparative study with the backstepping technique, demonstrating the effectiveness of the suggested solution. The results have been validated by numerical simulation within MATLAB/Simulink power systems environment.

Corresponding Author:

Fatim-Zahra Zaghar
LIMAT Lab, Faculty of Sciences Ben M'sick, Hassan II University
BP 7955 Casablanca, Morocco
Email: fatizaghar@gmail.com

1. INTRODUCTION

Nowadays, boost converters have become popular in power supplies, battery-powered devices and specially in renewable energy applications such as solar power. The boost converters are used to manage and convert the varying DC voltages generated by solar panels into a stable output suitable for use or storage [1]–[5]. These converters are nonlinear, which makes the control strategies challenging. Electrical engineering has seen significant advancements in DC-DC converter regulation, utilizing various control methods, including proportional integrator and derivative (PID), fuzzy logic, fractional fuzzy PI controller using particle swarm optimization (PSO) [6], [7]. In studies [8], [9], authors used cascade proportional integrator and robust proportional-integrator-derivative (PID) controllers. However, the results showed a lower stability and delay in response time, particularly in different operating conditions. Sliding mode control methods [10], and robust PID controllers [11] were proposed to address these issues. Therefore, similar results have been achieved.

Nonlinear controllers, known for their robustness, have been explored to handle nonlinear systems. An innovative power boost converter introduced a switched-capacitor setup with a sliding mode controller to reduce voltage stress and enhance DC voltage gain [12]. In research [13], adaptive robust fuzzy PI control is designed. However, the controllers faced computational challenges that require further investigation. Traditional methods have many challenges on tracking the maximum power point, hence the necessity of using intelligent algorithms

that are well-suited for nonlinear systems. In research [14], the backstepping technique is used and proved effective in dealing with irradiation distortion and load imbalance. A sliding mode backstepping controller is applied for boost converter, the controller ensures the system's robustness [15]. In research [16], integral backstepping applied for a DC–DC three-level boost converters, the regulator results are outperforming over other controllers. On the AC side, an adaptive reference PI controller is introduced for the inverter to enhance the system's performance [17]. Additionally, authors in research [18] presented an integral backstepping control strategy for an inverter in an islanded micro-grid, demonstrating exceptional responsiveness. Furthermore, an integral backstepping control applied to enhance the power quality of micro-grid-connected PV system [19].

In the studies mentioned above, the focus has been on controlling the single-phase boost converter or studying the inverter in an islanded micro-grid. Others have been interested in studying the three-phase system by directly connecting the inverter to PV modules such in [20]–[23]. This topology has an inconvenience; the PV panel can be easily impacted by the grid fluctuations, which could affect its overall quality and performance. The use of a boost converter helps regulate and increase the voltage output from the solar panel, ensuring a more stable and reliable power supply to the inverter. This particularity leads us to study an overall three-phase system, including both converters (boost and inverter), using an intelligent method to improve the stability and response time during transient period.

The primary research objectives introduced an innovative nonlinear controller for the proposed system structure. Mainly, conventional backstepping and integral backstepping methods, tailored for boost converter to optimize the PV power output. This emphasized key points in DC-DC converter control, including voltage regulation, steady-state performance, nonlinear handling, and the effectiveness of the integral backstepping technique. Secondly, a PI controller is used to ensure the unit power factor correction. To the best of the authors' knowledge, this represents the initial formal assessment of both the proposed controller design and the system structure. The paper is organized as: i) Section 2 is dedicated to the discussion of the controller design; ii) Section 3 presents and discusses the numerical simulation; and iii) Section 4 draws some conclusions.

2.   CONTROLLERS DESIGN

The objective is to design a nonlinear backstepping and integral backstepping controller for the boost converter: Ensuring precise tracking of the converter's output voltage to the reference voltage generated by the P&O technique. Additionally, a PI controller is formulated to enhance the inverter's output waveform as shown in Figure 1.

2.1. Backstepping approach

Applying Kirchhoff's law to the circuit diagram and considering x_1, x_2, and μ represent the average model of v_{pv}, i_L, and u, respectively. The average model is expressed as in (1) and (2).

$$\dot{x}_1 = \frac{I_{pv}}{C} - \frac{x_2}{C} \tag{1}$$

$$\dot{x}_2 = \frac{x_1}{L} - \mu \frac{v_{bus}}{L} \tag{2}$$

Considering the average model of the boost converter, the reference voltage denoted as V_{-opt}. The error is subsequently determined as in (3).

$$e_1 = V_{-opt} - V_{pv} \tag{3}$$

Deriving the (3) and replacing V_{pv} by its average model, the resulting expression is as in (4).

$$\dot{e}_1 = \dot{V}_{-opt} - \frac{I_{PV}}{C} + \frac{x_2}{C} \tag{4}$$

The Lyapunov function is expressed by (5).

$$V_1 = \frac{1}{2} e_1^2 \tag{5}$$

Upon deriving the Lyapunov function, the resultant expression is as in (6).

$$\dot{V}_{-opt} - \frac{I_{PV}}{C} + \frac{x_2}{C} = - K_1 e_1 \tag{6}$$

To ensure system's stability, it is crucial for the Lyapunov function to exhibit positive definiteness, and its derivative should demonstrate negative definiteness (7), as cited in [24].

$$\dot{V}_1 = -k_1 e_1{}^2 \tag{7}$$

Second stage aims to track β reference current by establishing and error e_2 (8) and its derivative (9):

$$e_2 = \beta - \frac{x_2}{C} \tag{8}$$

$$\dot{e}_2 = \dot{\beta} - \frac{V_{pv}}{LC} + \frac{V_{bus}}{LC}(1-\mu) \tag{9}$$

To ensure the convergence of both errors, a composite Lyapunov function (V_c) and its derivative are defined respectively in (10) and (11):

$$V_c = V_1 + \frac{1}{2}e_2^2 \tag{10}$$

$$\dot{V}_c = -k_1 e_1{}^2 + e_2 \dot{e}_2 \tag{11}$$

Then, $\dot{e}_2$ is considered as in (12).

$$\dot{e}_2 = \dot{\beta} - \frac{V_{pv}}{LC} + \frac{V_{bus}}{LC}(1-\mu) - e_1 \tag{12}$$

Finally, the (13) α is employed to stabilize the boost converter:

$$\mu = 1 - \left[\frac{L.C}{V_{bus}}\left(-K_2 e_2 + e_1 - \dot{\beta}\right) + \frac{V_{PV}}{V_{bus}}\right] \tag{13}$$

2.2. Integral backstepping controller

The input signal α is utilized by the boost converter to keep the controlled output y at its designated reference level as expressed in (14), ensuring stability of the system.

$$y_{1ref} = \frac{\partial P_{mpp}}{\partial v_{pmpp}} = 0 \tag{14}$$

The definition of the tracking error and its derivative are outlined in (15) and (16).

$$\varepsilon_{P1} = y_1 - y_{1ref} = i_P + V_P \frac{\partial i_P}{\partial v_P} \tag{15}$$

$$\dot{\varepsilon}_{P1} = \frac{1}{C_p}\left(2\frac{\partial i_P}{\partial V_P} + V_P \frac{\partial^2 i_P}{\partial v_{p2}}\right)(i_{p-i_L}) \tag{16}$$

The integral action is formulated within (17).

$$\delta_P = \int_0^t y_1(Z) - y_{1ref}(Z)dz = \int_0^t i_p + V_P \frac{\partial i_p}{\partial v_p}dz \tag{17}$$

To enhance the controller's robustness, we implement the following improvements in (18).

$$V_{P1}(\varepsilon_{P1}, \delta_P) = \frac{1}{2}\varepsilon_{P1} + 2\frac{1}{2}\delta_P{}^2 \tag{18}$$

Afterward, we can represent the derivative of the improved controller as in (19).

$$\dot{V}_{P1}(\varepsilon_{P1}, \delta_P) = \varepsilon_{P1}\left[\delta_P + \frac{1}{C_p}\left(2\frac{\partial i_P}{\partial V_P} + V_P \frac{\partial^2 i_P}{\partial v_{p2}}\right)(i_{p-i_L})\right] \tag{19}$$

To stabilize tracking errors ε_{p1} and integral action δ_P, an artificial control is needed to maintain a desired boost inductor current value $\mu = (i_L)_d$, ensuring the negativity of the Lyapunov function derivative (as shown in (20)).

$$\delta_P + \frac{1}{C_p}\left(2\frac{\partial i_P}{\partial v_P} + V_P \frac{\partial^2 i_P}{\partial v_{p^2}}\right)(i_P - \mu) = C_{1P}\varepsilon_{P1} \tag{20}$$

Once $C_{1P} > 0$, an adjustment parameter is set at 10000, leading to the following outcome (21).

$$\mu = i_p + \frac{C_P}{2\frac{\partial i_P}{\partial v_P} + v_P\frac{\partial^2 i_P}{\partial v_{p2}}}(C_{1P}\varepsilon_{P1} + \delta_P) \tag{21}$$

Choosing the virtual controller leads to the Lyapunov function's derivative becoming negative (22).

$$\dot{V}_{p1} = -C_{1P}\varepsilon_{P1}{}^2 < 0 \tag{22}$$

In the next phase, we introduce a tracking error addressed as in (23).

$$\varepsilon_{P2} = i_L - \mu \tag{23}$$

By incorporating the (23) into the (19), the expression of $\dot{\varepsilon}_{P1}$ becomes:

$$\dot{\varepsilon}_{P1} = \frac{1}{C_P}\left(2\frac{\partial i_P}{\partial v_P} + v_P \frac{\partial^2 i_P}{\partial v_{p^2}}\right)(i_P - \varepsilon_{p2} - \mu) \tag{24}$$

Upon combining (21) and (24), we arrive at the following resulting expression:

$$\delta_P + \dot{\varepsilon}_{P1} = -C_{1P}\varepsilon_{P1} - \frac{1}{C_P}\left(2\frac{\partial i_P}{\partial v_P} + v_P \frac{\partial^2 i_P}{\partial v_{p^2}}\right)\varepsilon_{p2} \tag{25}$$

The second Lyapunov candidate function and its derivative are described in (26) and (27):

$$V_{P2}(\delta_p, \varepsilon_{P1}, \varepsilon_{p2}) = V_{P1} + \frac{1}{2}\varepsilon_{P2}{}^2 \tag{26}$$

$$\dot{V}_{P2}(\delta_p, \varepsilon_{P1}, \varepsilon_{p2}) = -C_{1P}\varepsilon_{P1}{}^2 + \varepsilon_{p2}\left[\dot{\varepsilon}_{P2} - \frac{1}{C_P}\left(2\frac{\partial i_P}{\partial v_P} + v_P \frac{\partial^2 i_P}{\partial v_{p^2}}\right)\varepsilon_{P1}\right] \tag{27}$$

Once more, the derivative of ε_{p2} is given by:

$$\dot{\varepsilon}_{P2} = \frac{di_L}{dt} - \dot{\mu} = \frac{1}{L}V_P - \frac{1}{L}(1-\alpha)V_{dc} - \dot{\mu} \tag{28}$$

The virtual controller's derivative can be represented as (29).

$$\dot{\mu} = \frac{\partial i_p}{\partial v_p}\frac{\partial v_p}{\partial t} + \frac{(c_1\dot{\varepsilon}_{P1} + \varepsilon_{P1})}{\left(2\frac{\partial i_P}{\partial v_P} + v_P\frac{\partial^2 i_P}{\partial v_{p^2}}\right)} - C_P \frac{(c_1\varepsilon_{P1} + \delta_p)}{\left(2\frac{\partial i_P}{\partial v_P} + v_P\frac{\partial^2 i_P}{\partial v_{p^2}}\right)} * \left(3\frac{\partial^2 i_P}{\partial v_{P2}} + V_P \frac{\partial^3 i_P}{\partial v_{p3}}\right)\frac{\partial v_p}{\partial t} \tag{29}$$

Through the substitution of the derived expression of $\dot{\varepsilon}_{P2}$ from (28) into (29), the result is as in (30).

$$\dot{V}_{P2}(\delta_p, \varepsilon_{P1}, \varepsilon_{p2}) = -C_{1P}\varepsilon_{P1}{}^2 + \varepsilon_{p2}\left[\frac{1}{L}V_P - \frac{1}{L}(1-\alpha)V_{dc} - \dot{\mu} - \frac{1}{C_P}\left(2\frac{\partial i_P}{\partial v_P} + v_P \frac{\partial^2 i_P}{\partial v_{p^2}}\right)\varepsilon_{P1}\right] \tag{30}$$

The control input α is formulated as in (31).

$$\alpha = \frac{L}{V_{dc}}\left[-C_{2P}\varepsilon_{P2} + \frac{1}{C_P}\left(2\frac{\partial i_P}{\partial v_P} + v_P \frac{\partial^2 i_P}{\partial v_{p^2}}\right)\varepsilon_{P1} - \frac{1}{L}(V_P - V_{dc}) + \dot{\mu}\right] \tag{31}$$

With C_{2P} set as a positive constant, particularly at 10000, $\dot{V}_{P2}$ is negative and can be expressed as in (32).

$$\dot{V}_{P2} = -c_{1P}\varepsilon_{P1}{}^2 - C_{2P}\varepsilon_{P2}{}^2 < 0 \tag{32}$$

2.3. PI Controller

　　　　The design of the inverter controller comprises multiple interconnected blocks, each serving specific functions, which are described as: i) PLL block: To determine the grid voltage angle, a three-phase phase-locked loop (PLL) module is employed to produce three-phase signal characterized by frequency $\omega t_{,}$, this frequency serve a crucial role in producing the currents in the dq_1 frame; and ii) The "abc$_1$to dq0$_1$" block: This particular module is accountable for the conversion of the three-phase current signal, denoted as I_{abc}, into a dq0 rotating reference frame, represented as (I_d and I_q). The primary purpose of this module is to streamline the transformation process from the three-phase signal to the $dq0_1$ frame. Subsequently, a comparison is conducted between the converted current signal (I_d and I_q) and its reference values (I_{dref} and I_{qref}) employing the PI controllers' transfer function as shown in (33). In this scenario, I_{qref} is set to zero, as the focus is on attaining zero reactive power [25].

$$P + I.T_s \frac{1}{Z-1} \tag{33}$$

The value of parameters used for the controllers of the I_d and I_q are respectively $P_2 = 0.005$; $I_2 = 1$ and $P_3 = 0.005$; $I_3 = 1$ The discrepancies introduced by the controllers are then used to generate a modulation signal, which is utilized to control the inverter with the primary goal of achieving synchronization with the grid voltage.
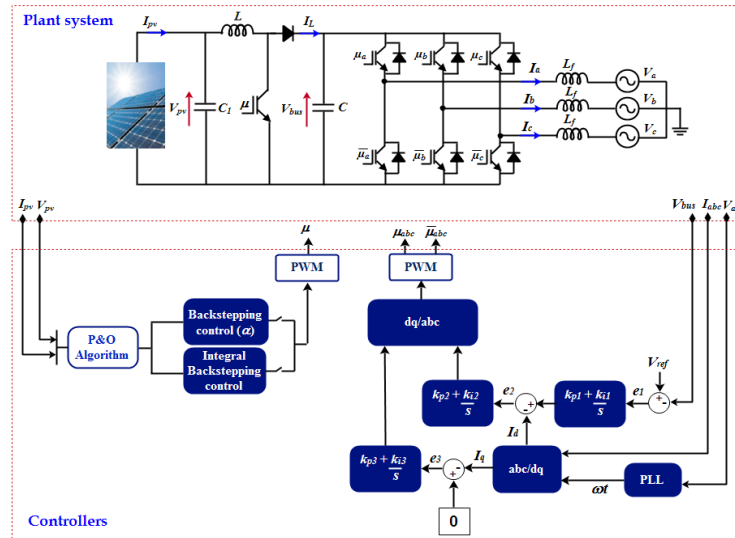

Figure 1. Diversity of controller applications in PV system

3.   RESULTS AND DISCUSSION

Within this portion, the efficiency of the suggested controllers trough numerical simulations. The characteristics of the system are detailed in Table 1. The simulation utilizes the irradiation profile illustrated in Figure 2 and the temperature profile depicted in Figure 3.

The study involved testing the controllers in different conditions, particularly focusing on varying levels of irradiation and temperature. The irradiation profile starts at zero and remains constant until t=0.4 s. It then steadily increases, reaching a peak of $1000\ W/m^2$ at approximately t≈ 2.25 s before gradually decreasing back to zero. These profiles are crucial for understanding how the controllers perform under environmental conditions. Figures 2 and 3 provide a representation of these changes over time.

Table 1. Electrical characteristics of the system

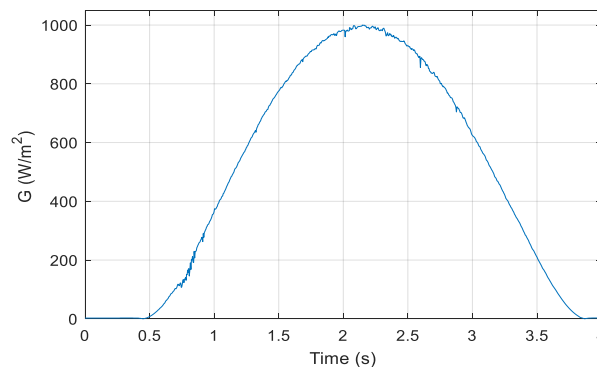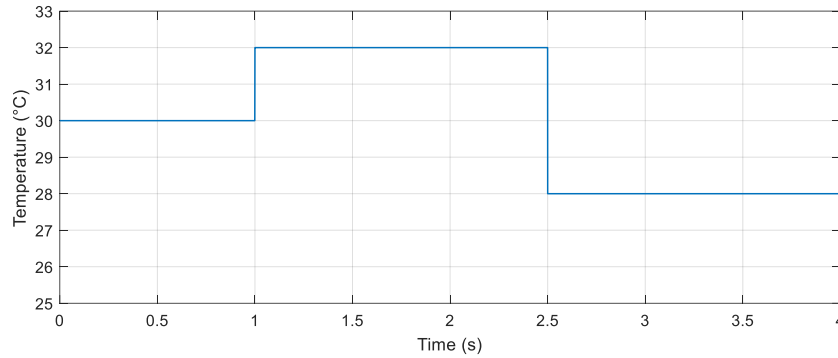| Parameter	Symbol	Value
Filter	L_f	0.0028
Photovoltaic system	N_s	14
	N_p	17
Boost converter	C_1	1e-04
	L_1	0.0016

Figure 2. Solar irradiation profile

Figure 3. Temperature profile

Figure 4 shows the dynamic performance of the conventional backstepping technique during photovoltaic voltage changes using the P&O algorithm, the change in input voltage shows a perturbation that goes from 340 V to 400 V. Then, it become stable until 3.9 s. Backstepping emphasizes its efficiency in diverse scenarios. However, we found out that the steady-state error is important at 3.9 s. Considering these results, to improve the steady-state error, we had studied the integral backstepping controller, the controller proposed highlights its strong dynamic capabilities of tracking, it exhibits minimal overshoot and achieves rapid recovery within a 3.9-second timeframe. The suggested control method effectively addresses voltage step changes in distributed power generation as shown in Figure 5.

The three-phase control system employs a PI mechanism, as seen in Figure 6, to effectively regulate the DC bus voltage, ensuring it aligns with the desired reference level. This utilization of the PI control not only achieves stable voltage control but also contributes to improve power factor correction. In Figure 7, we observe key characteristics of the reference current (I_{abc}) and voltage (V_{abc}). These characteristics provide valuable insights into the behavior of the control system and its ability to maintain desired current and voltage levels which is difficult to keep it maintained as the overall system contains three important blocks with non-linear controllers that were applied in parallel.

For a deeper understanding of the control system's performance, Figure 8 offers detailed information on the power-voltage (P-V) characteristics, specifically P_{pv} and P_{mpp} curves. These curves are important in assessing MPPT performance. Remarkably, the P_{mpp} curve closely follows the irradiation curve, indicating an outstanding MPPT performance. This alignment signifies the system's efficiency in optimizing power output in response to varying irradiation levels.

Reactive power (Q_{inv}) in the study has been regulated to zero to maintain the current and voltage in phase and ensure a good power factor. The active power (P_{inv}) represents the actual power consumed or generated by the system. The injected active power reaches 50 Mw. Taking the average during the period of [2s-2.5s], the energy injected is equal to 0.41 Mwh. Both powers are represented in Figure 9.

Figure 10 illustrated overall distortion due to harmonics, showing a progressive decrease as transmitted power increased, stabilizing at 3%. This achievement aligns well with the IEEE 512-1992 standard of 5% for total harmonic distortion. Further reduction in distortion, potentially involving increased filter values, is possible, but must be approached cautiously to preserve operational efficiency.
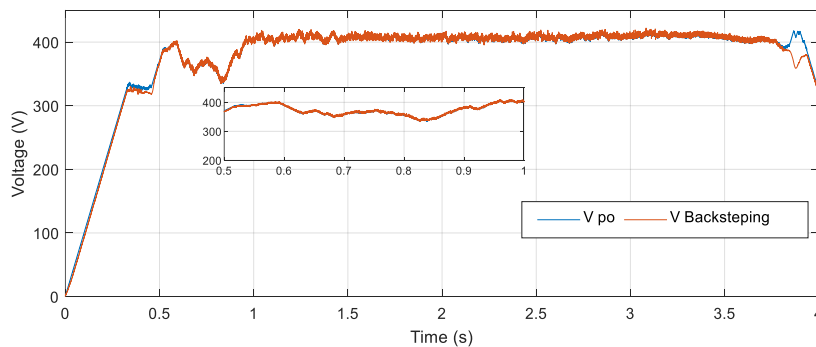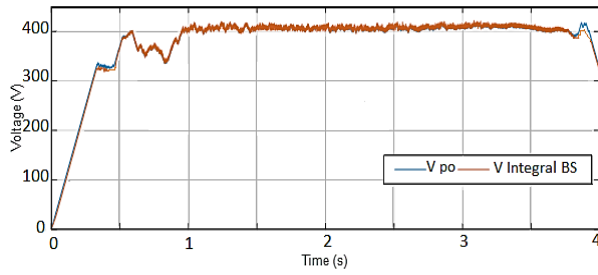

Figure 4. V_{bus} by applying backstepping

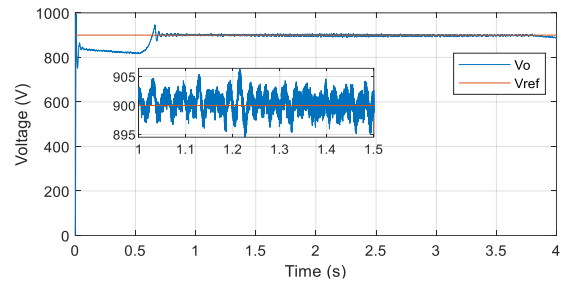Figure 5. V_{bus} by applying integral backstepping
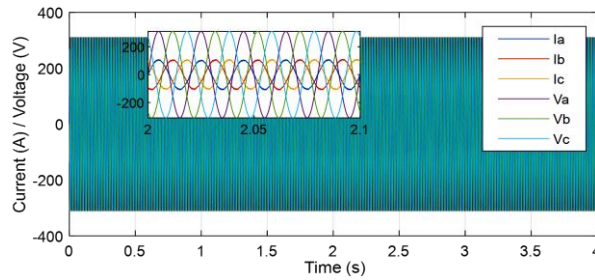

Figure 6. DC link output voltage

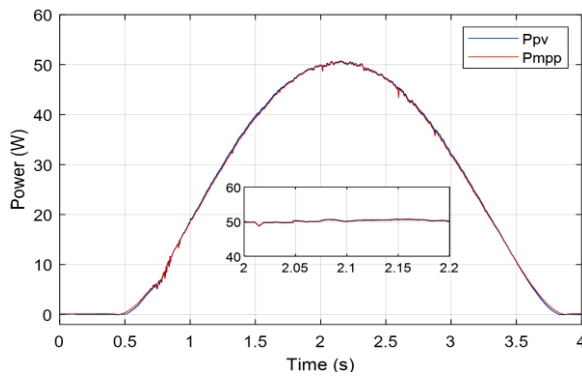Figure 7. I_{abc} and V_{abc} curves

Figure 8. P_{mpp} and P_{pv} graphs
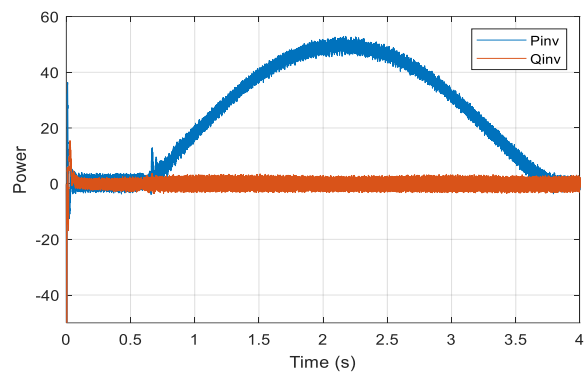

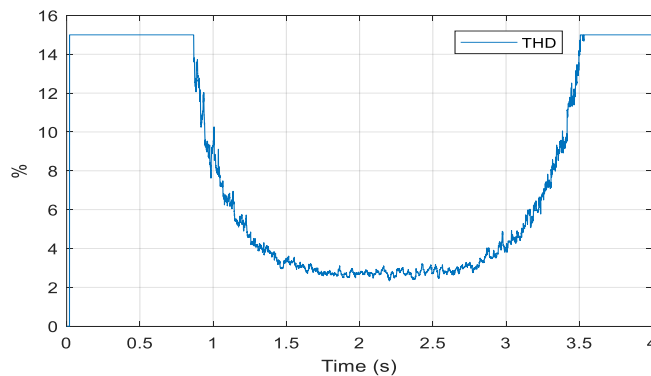Figure 9. P_{inv} and Q_{inv} graphs

Figure 10. Total harmonic distortion graph

4.   CONCLUSION

The present study addresses the problem of controlling a three-phase double stage topology of electrical grid connected photovoltaic system. A nonlinear controller is developed, utilizing both conventional

backstepping and integral backstepping techniques to guarantee the stability of the system's large signals. The designed outer loop provides optimal results, particularly in minimizing steady-state errors in the DC bus voltage arising from mismatch interference, input voltage variations, and model uncertainty. The dynamic performance is satisfactory, and the controller parameters meticulously designed using Lyapunov stability conditions to ensure the overall global stability.

A comparative study of the proposed method is conducted. The results have been verified through numerical simulation using the MATLAB/Simulink. According to the aforementioned findings, it is evident that the suggested control exhibits favorable performance in settling time, startup, and overshoot, indicating enhanced robustness and dynamism.

The designed inner loop achieves low total harmonic distortion, and the analysis reveals that the active power transfer (P_{inv}) demonstrates a similar trend to the P_{pv} power curve. Moreover, it is observed that there is no injection of reactive power (Q_{inv}) into the grid, indicating the satisfactory performance of both the inverter and boost controls. These conclusions are supported by the results of the total harmonic distortion (THD) analysis.

REFERENCES

[1] S. Hemalatha, A. J. Renoald, G. Banu, and K. Indirajith, "Design and investigation of PV string/central architecture for bayesian fusion technique using grey wolf optimization and flower pollination optimized algorithm," *Energy Conversion and Management*, vol. 286, 2023, doi: 10.1016/j.enconman.2023.117078.

[2] A. Hayat, D. Sibtain, A. F. Murtaza, S. Shahzad, M. S. Jajja, and H. Kilic, "Design and Analysis of Input Capacitor in DC–DC Boost Converter for Photovoltaic-Based Systems," *Sustainability (Switzerland)*, vol. 15, no. 7, 2023, doi: 10.3390/su15076321.

[3] S. Nagaraja Rao, S. K. Anisetty, B. M. Manjunatha, B. M. Kiran Kumar, V. Praveen Kumar, and S. Pranupa, "Interleaved high-gain boost converter powered by solar energy using hybrid-based MPP tracking technique," *Clean Energy*, vol. 6, no. 3, pp. 460–475, 2022, doi: 10.1093/ce/zkac026.

[4] S. Chen *et al.*, "Research on topology of the high step-up boost converter with coupled inductor," *IEEE Transactions on Power Electronics*, vol. 34, no. 11, pp. 10733–10745, 2019, doi: 10.1109/TPEL.2019.2897871.

[5] M. Villegas-Ruvalcaba, K. J. Gurubel-Tun, and A. Coronado-Mendoza, "Robust inverse optimal control for a boost converter," *Energies*, vol. 14, no. 9, 2021, doi: 10.3390/en14092507.

[6] A. Rajavel and N. R. Prabha, "Fuzzy logic controller-based boost and buck-boost converter for maximum power point tracking in solar system," *Transactions of the Institute of Measurement and Control*, vol. 43, no. 4, pp. 945–957, 2021, doi: 10.1177/0142331220938211.

[7] M. Demirtas and F. Ahmad, "Fractional fuzzy PI controller using particle swarm optimization to improve power factor by boost converter," *International Journal of Optimization and Control: Theories and Applications*, vol. 13, no. 2, pp. 205–213, 2023, doi: 10.11121/ijocta.2023.1260.

[8] C. Yanarates and Z. Zhou, "Design and Cascade PI Controller-Based Robust Model Reference Adaptive Control of DC-DC Boost Converter," *IEEE Access*, vol. 10, pp. 44909–44922, 2022, doi: 10.1109/ACCESS.2022.3169591.

[9] T. Kobaku, R. Jeyasenthil, S. Sahoo, and T. Dragicevic, "Experimental Verification of Robust PID Controller under Feedforward Framework for a Nonminimum Phase DC-DC Boost Converter," *IEEE Journal of Emerging and Selected Topics in Power Electronics*, vol. 9, no. 3, pp. 3373–3383, 2021, doi: 10.1109/JESTPE.2020.2999649.

[10] J. Rivera, S. Ortega-Cisneros, J. C. Rosas-Caro, and O. F. Ruíz-Martínez, "Sliding Mode Regulation of a Boost Circuit for DC-Biased Sinusoidal Power Conversion," *Applied Sciences (Switzerland)*, vol. 13, no. 10, 2023, doi: 10.3390/app13105963.

[11] T. Kobaku, R. Jeyasenthil, S. Sahoo, R. Ramchand, and T. Dragicevic, "Quantitative Feedback Design-Based Robust PID Control of Voltage Mode Controlled DC-DC Boost Converter," *IEEE Transactions on Circuits and Systems II: Express Briefs*, vol. 68, no. 1, pp. 286–290, 2021, doi: 10.1109/TCSII.2020.2988319.

[12] Q. Qi, D. Ghaderi, and J. M. Guerrero, "Sliding mode controller-based switched-capacitor-based high DC gain and low voltage stress DC-DC boost converter for photovoltaic applications," *International Journal of Electrical Power and Energy Systems*, vol. 125, 2021, doi: 10.1016/j.ijepes.2020.106496.

[13] V. Kumar, A. Mitra, O. Shaklya, S. Sharma, and K. P. S. Rana, "An adaptive robust fuzzy PI controller for maximum power point tracking of photovoltaic system," *Optik*, vol. 259, 2022, doi: 10.1016/j.ijleo.2022.168942.

[14] M. Moutchou and A. Jbari, "Fast photovoltaic IncCond-MPPT and backstepping control, using DC-DC boost converter," *International Journal of Electrical and Computer Engineering*, vol. 10, no. 1, pp. 1101–1112, 2020, doi: 10.11591/ijece.v10i1.pp1101-1112.

[15] R. N. Deo, A. Shrivastava, and K. Chatterjee, "Implementation of sliding mode backstepping controller for boost converter in real-time for LED application," *Expert Systems*, vol. 40, no. 6, 2023, doi: 10.1111/exsy.13095.

[16] I. A. Ayad *et al.*, "Optimized Nonlinear Integral Backstepping Controller for DC-DC Three-Level Boost Converters," *IEEE Access*, vol. 11, pp. 49794–49805, 2023, doi: 10.1109/ACCESS.2023.3274773.

[17] A. Alhejji and M. I. Mosaad, "Performance enhancement of grid-connected PV systems using adaptive reference PI controller," *Ain Shams Engineering Journal*, vol. 12, no. 1, pp. 541–554, 2021, doi: 10.1016/j.asej.2020.08.006.

[18] A. A. Shah, X. Han, H. Armghan, and A. A. Almani, "A nonlinear integral backstepping controller to regulate the voltage and frequency of an islanded microgrid inverter," *Electronics (Switzerland)*, vol. 10, no. 6, pp. 1–24, 2021, doi: 10.3390/electronics10060660.

[19] N. Debdouche, L. Zarour, H. Benbouhenni, F. Mehazzem, and B. Deffaf, "Robust integral backstepping control microgrid connected photovoltaic System with battery energy storage through multi-functional voltage source inverter using direct power control SVM strategies," *Energy Reports*, vol. 10, pp. 565–580, 2023, doi: 10.1016/j.egyr.2023.07.012.

[20] Z. Hekss, A. Abouloifa, I. Lachkar, F. Giri, S. Echalih, and J. M. Guerrero, "Nonlinear adaptive control design with average performance analysis for photovoltaic system based on half bridge shunt active power filter," *International Journal of Electrical Power and Energy Systems*, vol. 125, 2021, doi: 10.1016/j.ijepes.2020.106478.

[21] J. R. Albert *et al.*, "Investigation on load harmonic reduction through solar-power utilization in intermittent SSFI using particle swarm, genetic, and modified firefly optimization algorithms," *Journal of Intelligent and Fuzzy Systems*, vol. 42, no. 4, pp. 4117–4133, 2022, doi: 10.3233/JIFS-212559.

[22] J. R. Albert, "Design and Investigation of Solar PV Fed Single-Source Voltage-Lift Multilevel Inverter Using Intelligent Controllers," *Journal of Control, Automation and Electrical Systems*, vol. 33, no. 5, pp. 1537–1562, 2022, doi: 10.1007/s40313-021-00892-w.

[23] M. Aourir, A. Abouloifa, I. Lachkar, C. Aouadi, F. Giri, and J. M. Guerrero, "Nonlinear control and stability analysis of single stage grid-connected photovoltaic systems," *International Journal of Electrical Power and Energy Systems*, vol. 115, 2020, doi: 10.1016/j.ijepes.2019.105439.

[24] O. Diouri, N. Es-Sbai, F. Errahimi, A. Gaga, and C. Alaoui, "Modeling and Design of Single-Phase PV Inverter with MPPT Algorithm Applied to the Boost Converter Using Back-Stepping Control in Standalone Mode," *International Journal of Photoenergy*, vol. 2019, 2019, doi: 10.1155/2019/7021578.

[25] A. Althobaiti, N. Ullah, Y. Belkhier, A. Jamal Babqi, H. I. Alkhammash, and A. Ibeas, "Expert knowledge based proportional resonant controller for three phase inverter under abnormal grid conditions," *International Journal of Green Energy*, vol. 20, no. 7, pp. 767–783, 2023, doi: 10.1080/15435075.2022.2107395.

BIOGRAPHIES OF AUTHORS

Fatim-Zahra Zaghar received an Engineering degree in electrical engineering, electronics and telecommunication from Mohamed VI international academy of civil aviation Casablanca in 2017. She is currently pursuing the Ph.D. degree in physics and applications ate faculty of sciences Ben M'sik, Hassan II University of Casablanca. My research interests revolve around renewable energy systems, application of nonlinear control techniques to boost converters, and enhancing power quality in electrical energy. She can be contacted at email: fatizaghar@gmail.com.

Zineb Hekss received a Master's degree in Data Processing from the Faculty of Sciences Ben M'sick, Hassan II University of Casablanca, in 2017, and the Ph.D. degree in Electrical Engineering and automatic control from the National Higher School of Electricity and Mechanics (ENSEM), Hassan II University of Casablanca, Morocco, in 2022. She is currently a Professor at Moroccan school of engineering. Her research interests include renewable energy systems, power quality. She can be contacted at email: zineb.hekss-etu@etu.univh2c.ma.

Mohamed Rafi is currently a professor of engineering sciences in general and materials physics and applications of renewable energies in particular at the Mohammed VI International Academy of Civil Aviation. He has expertise in the performance of photovoltaic systems. His expertise is highly sought after in the case of ternary and quaternary materials used in thin layers. He is interested in modeling, design, prediction, and simulation problems of smart grid. He obtained His Ph.D. in Materials Science and Engineering and his HDR in Renewable Energy. He can be contacted at email: rafi3mhd@gmail.com.

Salwa Echalih received a Master's degree in Data Processing from the Faculty of Sciences Ben M'sik, Hassan II University of Casablanca, Morocco, in 2017, and the Ph.D. degree in Electrical Engineering from the National Higher School of Electricity and Mechanics (ENSEM), Hassan II University of Casablanca, Morocco, in 2022. Her research interests include renewable energy systems, power quality, modeling, observation, and nonlinear control techniques of active power filter. She can be contacted at email: salwa.echalih-etu@etu.univh2c.ma.

Abderraouf Ridah is a full professor of materials physics and applications at University of Hassan II, Casablanca, Morocco. He has expertise in renewable Energy, Photovoltaics including: Solar Cells, Thin Films Technology and Nanotechnology, Material Characterization, Thin Film Deposition Materials and Semiconductor Device Physics. He can be contacted at email: abderraoufridah@yahoo.fr.